

Blue supergiants as descendants of magnetic main sequence stars

I. Petermann, N. Langer, N. Castro, and L. Fossati

Argelander Institut für Astronomie der Universität Bonn, Auf dem Hügel 71, 53121 Bonn, Germany
e-mail: ipeterma@asu.edu

Received 13 April 2015 / Accepted 5 July 2015

ABSTRACT

About 10% of the massive main sequence stars have recently been found to host a strong, large scale magnetic field. Both, the origin and the evolutionary consequences of these fields are largely unknown. We argue that these fields may be sufficiently strong in the deep interior of the stars to suppress convection near the outer edge of their convective core. We performed parametrised stellar evolution calculations and assumed a reduced size of the convective core for stars in the mass range $16 M_{\odot}$ to $28 M_{\odot}$ from the zero age main sequence until core carbon depletion. We find that such models avoid the coolest part of the main sequence band, which is usually filled by evolutionary models that include convective core overshooting. Furthermore, our “magnetic” models populate the blue supergiant region during core helium burning, i.e., the post-main sequence gap left by ordinary single star models, and some of them end their life in a position near that of the progenitor of Supernova 1987A in the Hertzsprung-Russell diagram. Further effects include a strongly reduced luminosity during the red supergiant stage, and downward shift of the limiting initial mass for white dwarf and neutron star formation.

Key words. stars: massive – supergiants – stars: magnetic field – stars: evolution – supernovae: individual: SN 1987A

1. Introduction

Massive stars are important cosmic engines, because they drive the evolution of star forming galaxies (Mac Low et al. 2005), and are very bright and thus visible from very long distances (Kudritzki et al. 2008). Nevertheless, even their longest lasting evolutionary stage, core hydrogen burning, has not yet been understood well. While one of the two culprits, mass loss, strongly affects only the very massive stars, it is the other one, internal mixing processes, that still leads to many questions. This refers to thermally driven mixing as caused by convection, overshooting, or semiconvection as well as to rotationally induced mixing and the mixing affected by magnetic fields.

In recent years, it has become evident that the concept of considering one evolutionary path for stars of a given mass fails in the massive star regime. Hunter et al. (2008) and Brott et al. (2011) show that early B-type main sequence stars fall into several distinctly different categories, as classified by their spin and surface nitrogen abundance. Dufton et al. (2013) show that the rotational velocity distribution of Large Magellanic Cloud (LMC) early B stars is bimodal, similar to late B and A stars (Royer et al. 2007). The physical reasons for this are not clear yet, but could relate to initial rotation, binarity, and strong internal magnetic fields (Langer 2012).

In the present paper, we consider one of the least investigated aspects of massive star evolution, namely the effects of internal magnetic fields. Four different types of magnetic fields in massive stars have been discussed in recent years. First, there is the idea that differential rotation in their radiative envelopes produces toroidal fields through a dynamo process (Spruit 2002). While the functioning of this dynamo is still being debated (Zahn 2011), asteroseismic measurements in red giants (Mosser et al. 2012) call for a strong angular momentum transport mechanism which could be provided by this predominantly toroidal field (Suijs et al. 2008; Heger et al. 2005). This type of field, which

would not be directly observable, and its consequences would be as ubiquitous as differential rotation.

Second, massive stars have convective cores, and it appears likely that an $\alpha\Omega$ -dynamo can produce a magnetic field in these cores. In fact, the magnetohydrodynamic (MHD) simulations of Brun et al. (2005) show the functioning of such a dynamo in the convective cores of even slowly rotating $2 M_{\odot}$ stars, where the field growths saturate near their equipartition values. MacGregor & Cassinelli (2003) show that this field is unlikely to rise to the surface of the star during its lifetime, so again, it may not be directly observable. Its effects in the vicinity of the convective core are largely unexplored.

A third type of magnetic field in massive stars has been suggested by Cantiello et al. (2009), who propose that an $\alpha\Omega$ -dynamo may work in their iron opacity driven sub-surface convection zones. The produced flux tubes could then buoyantly float to the stellar surface and produce magnetic spots (Cantiello & Braithwaite 2011), which may be observationally indicated by the moving discrete absorption components in the UV resonance lines found in O-star spectra (Prinja & Howarth 1988; Kaper et al. 1997).

Here we are concerned with a fourth type of magnetic field in massive stars, namely strong large scale fields that are anchored in the radiative stellar envelope and that form an observable magnetosphere outside the star. Only OB stars with such fields will be designated as magnetic OB stars in this paper. Until recently, only three magnetic O-type stars were known, HD 37022 (Donati et al. 2002), HD 191612 (Donati et al. 2006) and ξ Orionis A (Bouret et al. 2008). However, new intense searches have revealed many more magnetic OB stars (Grunhut et al. 2009; Petit et al. 2013; Hubrig et al. 2013, 2014), thus implying an incidence fraction of strong, large scale B-fields in OB stars of about ten percent (Grunhut & Wade 2012).

In contrast to the first three types of magnetic fields in OB stars, which all need a dynamo process to continuously

produce the field because it would quickly decay otherwise, the strong large scale fields are thought to be stable for two reasons. First, they occur mostly in very slow rotators and in stars with radiative envelopes, such that there is no known dynamo process that could produce them. Second, Braithwaite & Spruit (2004) find that magnetic field configurations resembling the ones observed in magnetic OB stars can indeed be stable, in the sense that their decay may take longer than the stellar lifetime.

The origin of these stable, large-scale magnetic fields in massive stars is mainly described by two ideas. The hypothesis of fossil fields (Braithwaite & Nordlund 2006) assumes that magnetic fields in a molecular cloud are conserved during star formation. It is, however, difficult to explain, why only a low percentage of stars preserves a magnetic field in this formation channel. The effects of a fossil magnetic field on convective core dynamo in A-type stars are described in Featherstone et al. (2009).

Magnetic stars can also be the result of strong binary interaction (Langer 2014). For example, they could be the product of the merger of two main sequence stars, which occurs quite frequently because a large number of massive stars have close companion stars (Sana et al. 2012). Garcia-Berro et al. (2012) show that strong magnetic fields can form in the hot, convective, differentially rotating envelope of a merger product of two white dwarfs, which may occur similarly in the case of a main sequence merger. Calculations by de Mink et al. (2014) suggest that among the galactic early-type stars, $8_{-4}^{+9}\%$ are the products of a merger event from a close binary system. The order of magnitude obtained in this study agrees well with the occurrence of magnetic massive stars. Furthermore, that many magnetic OB stars are nitrogen-enriched at their surface complies well with the models of merger stars by Glebbeek et al. (2013).

The evolutionary consequences of strong large scale magnetic fields in the stellar interior are largely unexplored. Most observed magnetic stars rotate slowly, such that rotational mixing plays no role at least at the present time. Furthermore, it is found that in many situations, large scale magnetic fields and convection repulse each other (e.g., Gough & Tayler 1966; Galloway & Weiss 1981). Therefore, while in evolutionary models of massive stars it is usually assumed that the convective core is extended over its standard size during core hydrogen burning (Brott et al. 2011; Ekström et al. 2012), we assume the opposite in the present paper, which means that internal large scale magnetic fields restrict the convective core to a smaller region than what the Ledoux criterion for convection would predict. We elaborate our assumptions and the computational method in Sect. 2, and present our evolutionary calculations in Sect. 3. After a comparison with observations in Sect. 4 we give our conclusions in Sect. 5.

2. Method

Our stellar models are calculated with a hydrodynamic stellar evolution code, which is described in detail in Yoon et al. (2006) and Köhler et al. (2015).

Convection is modelled using the Ledoux criterion, assuming a mixing-length parameter $\alpha_{\text{MLT}} = 1.5$ (Langer 1991). Semiconvection is implemented as described by Langer et al. (1983), applying a value of $\alpha_{\text{sem}} = 0.01$ (Langer 1991; see also Zaussinger & Spruit 2013). The description for mass loss follows Vink et al. (2000) for main sequence stars and blue supergiants, and Nieuwenhuijzen et al. (1990) for red supergiants. For our models we adopt solar abundances as the initial composition as in Brott et al. (2011).

The observed fields in magnetic massive stars are large scale fields, and while some of them have a more complex geometry many have a dominant dipole component (Donati & Landstreet 2009). Braithwaite & Spruit (2004) show that in order to achieve a stable magnetic field configuration, a dipole field needs to be balanced by an internal toroidal field. While a typical value for the observable part of the dipole field is 1 kG (Fossati et al. 2015), magnetic flux conservation would then predict field strength of up to 10^6 G near the convective core of a massive star. Additionally, Braithwaite (2009) has shown that the toroidal component can have a much higher field strength in a stable configuration than the poloidal component. Therefore, field strength of the order of 10^8 G cannot be excluded in the deep interior of magnetic massive stars and this corresponds to the equipartition field strength and indicates direct dynamical effects of the magnetic field on the convective motions.

Additionally, Zahn (2009) has shown that the magnetic field strength that is required to suppress convection is about two orders of magnitude less than the equipartition field strength, when thermal and Ohmic diffusion are taken into account. Zahn argues that this effect is observationally confirmed by the presence of sunspots and by surface inhomogeneities in Ap/Bp stars. We therefore assume in the following that convection near the boundary of the convective core is suppressed in magnetic massive stars.

Lydon & Sofia (1995) have suggested a modification of the stellar structure equations to account for the presence of a large scale magnetic field inside a star (see also Feiden & Chaboyer 2012). In our models, we ignore the changes induced by B fields on the structure of the star, which implies that we assume that the magnetic energy density is lower than the thermal energy density. We conduct a simple parametric study of stellar evolution models here with a diminished core mass compared to what is predicted by the Ledoux criterion for convection. To this end, we applied a modified Ledoux criterion as

$$\nabla_{\text{rad}} < f * \nabla_{\text{Led}}, \quad (1)$$

where

$$\nabla_{\text{Led}} = \nabla_{\text{ad}} - \frac{\chi_{\mu}}{\chi_T} \nabla_{\mu}. \quad (2)$$

Whereas this mimics the convection criterion to some extent in the presence of a vertical magnetic field proposed by Gough & Tayler (1966; see also Schatten & Sofia 1981; Tayler 1986), a quantitative prediction of the suppressive effects of large scale fields upon convection requires multi-dimensional MHD calculations. We thus refrain from relating our parameter f to magnetic field strengths, but make a heuristic choice for its values between 1.12 and 1.20, which leads to a reduction of the convective core mass of the order of 15% in our models. We restricted this change to the core hydrogen-burning phase, because the interactions of the magnetic field with the helium-burning core are uncertain. In particular, it remains unclear whether a significant fraction of the magnetic field will survive below the hydrogen-burning shell source.

At present, the origin of the large scale fields in massive stars is not clear (Langer 2014). While it might exist throughout core hydrogen burning if the field was inherited from the star formation process, it would be present for a fraction of that time if it was created in a binary merger or mass transfer process. However, a significant mass gain is expected to rejuvenate the star, that is to say that the binary interaction resets its evolutionary clock. Even though the time is not reset to zero in this case,

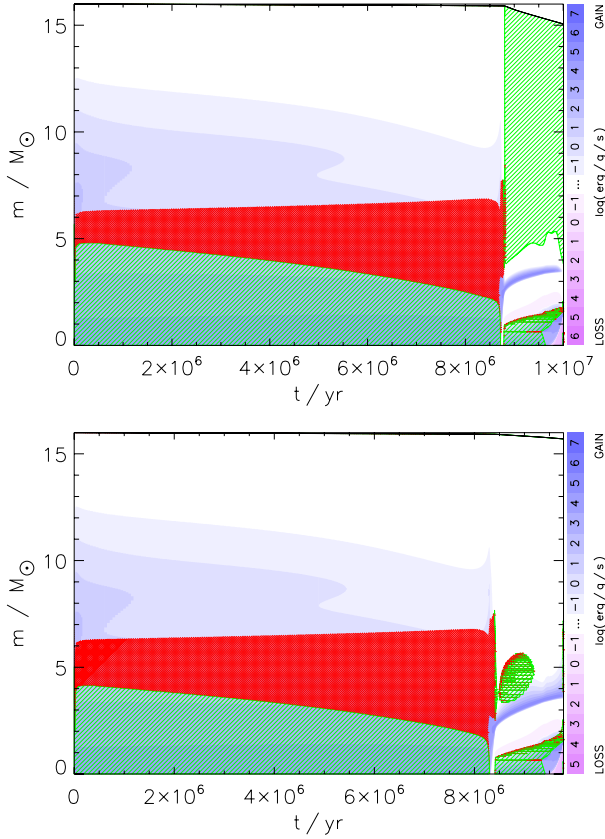


Fig. 1. Kippenhahn diagrams of two $16 M_{\odot}$ models computed with a convective core reduction parameter of $f = 1.12$ (top) and $f = 1.20$ (bottom). Convective (green) and semiconvective (red) regions are shown as a function of mass coordinate and time. Thermonuclear energy generation or loss is colour-coded as shown on the scale on the right-hand side. The evolutionary tracks of both models in the HR diagram are shown in Fig. 2.

we assume that the effect of a magnetic field decreasing the convective core is unaltered since the beginning of core hydrogen burning in our models.

All our models are evolved through core carbon burning, such that their presupernova positions in the Hertzsprung-Russell (HR) diagram can be reliably predicted.

3. Results

We performed calculations for stars in the mass range 16 to $28 M_{\odot}$, assuming different values for the convective core reduction parameter f (cf., Eq. (1)), and Table 1 gives an overview of the computed sequences. Figure 1 provides Kippenhahn diagrams showing the internal evolution of two $16 M_{\odot}$ star as an example, where reduction parameters $f = 1.12$ (top) and $f = 1.20$ (bottom) have been adopted. The convective cores are initially 5% and 18% lower in mass than for a non-reduced core, which leads to initial helium core masses of $2.4 M_{\odot}$ and $2.1 M_{\odot}$, in both cases, compared to $2.9 M_{\odot}$ for the unreduced case.

As shown in Fig. 1, extended semiconvective shells develop on top of the convective cores for the models with $f > 1$. While the interaction of these semiconvective layers with the large scale magnetic field is unclear, it is likely that the field also inhibits any semiconvection. For our simulations, this would make little difference, since the chosen small semiconvective efficiency parameter (see Sect. 2) means that there is very little chemical or energy transport in these zones.

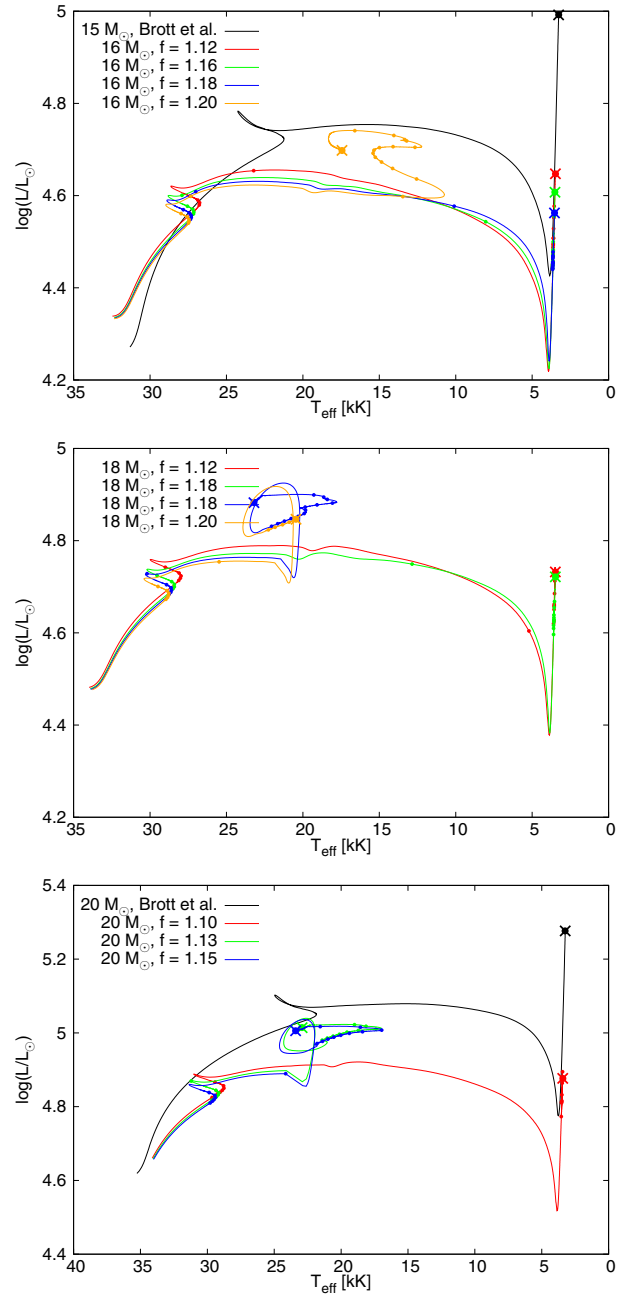


Fig. 2. Evolutionary tracks of stars with $M = 16, 18$ and $20 M_{\odot}$, computed with different core reduction parameters as indicated, in the HR diagram. For the post main sequence phases, small dots are placed on the tracks every 105 yr to indicate the speed of evolution of the models in the HR diagram. The large circle indicates the presupernova position of the models. For comparison, tracks for 15 and $20 M_{\odot}$ stars of non-rotating models with solar metallicity by Brott et al. (2011) are also shown.

The two stars shown in Fig. 1 develop helium cores of initially about $2.6 M_{\odot}$ ($f = 1.12$) and $2.2 M_{\odot}$ ($f = 1.20$), respectively, which increase to a final mass of about $3.5 M_{\odot}$ during core helium burning. Such values are expected in stars in the mass range $11 M_{\odot}$ to $12 M_{\odot}$ for the physics used in the models of Brott et al. (2011), that is, relatively large convective core overshooting.

Figure 2 (top) shows the evolutionary tracks of both $16 M_{\odot}$ models in the HR diagram. The minimum effective temperature during core hydrogen burning is higher for the model with the larger core reduction parameter, but both are very high compared

Table 1. Key quantities of the computed evolutionary models.

Acronym	M_i M_\odot	f	$M_{cc,i}$ M_\odot	$M_{He,i}$ M_\odot	$M_{He,f}$ M_\odot	τ_H Myr	τ_{He} Myr	$T_{eff,f}$ kK	$\log(L_f/L_\odot)$
M16f1.12	16	1.12	4.8	2.41	3.83	8.75	1.22	3.48	4.65
M16f1.16	16	1.16	4.4	2.27	3.77	8.56	1.36	3.51	4.61
M16f1.18	16	1.18	4.3	2.13	3.61	8.46	1.43	3.54	4.56
M16f1.20	16	1.20	4.1	2.12	3.52	8.37	1.37	17.4	4.70
M18f1.12	18	1.12	5.7	2.90	4.53	7.56	0.94	3.48	4.73
M18f1.16	18	1.16	5.2	2.68	4.44	7.38	1.04	3.49	4.72
M18f1.18	18	1.18	5.1	2.58	3.73	7.30	1.33	23.2	4.88
M18f1.20	18	1.20	5.0	2.40	3.32	7.21	1.46	20.5	4.85
M20f1.10	20	1.10	7.0	3.46	5.39	6.78	0.71	3.43	4.88
M20f1.13	20	1.13	6.5	3.28	4.33	6.66	0.92	22.9	5.01
M20f1.15	20	1.15	6.2	3.14	4.15	6.57	1.00	23.4	5.01
M22f1.18	22	1.18	7.0	3.36	4.30	5.82	0.93	24.6	5.10
M24f1.18	24	1.18	7.9	3.86	5.36	5.32	0.65	25.1	5.16
M28f1.18	28	1.18	10.0	4.76	6.54	4.61	0.50	24.7	5.31

Notes. Columns: acronym of the sequence, initial mass M_i , core reduction parameter f , the initial mass of the convective core $M_{cc,i}$, initial and final helium core masses $M_{He,i}$ and $M_{He,f}$, lifetimes of core hydrogen and core helium burning τ_H and τ_{He} , and presupernova effective temperature $T_{eff,f}$, and luminosity L_f .

to that of a model by Brott et al. (2011) shown in the same plot. Further on, the tracks in Fig. 2 show that the model computed with $f = 1.20$ never evolves into a red supergiant. Instead, its lowest effective temperature is about 10 000 K, and it ends its evolution at about 17 000 K, which is close to the effective temperature of the progenitor of Supernova 1987A. The $16 M_\odot$ model computed with $f = 1.12$, on the other hand, moves to the red supergiant branch quickly after core hydrogen exhaustion, and remains there for the rest of its evolution. Its luminosity during core helium burning and its presupernova luminosity of $\log L/L_\odot \simeq 4.65$ is much lower than the luminosity of models that assume convective core overshooting.

3.1. Variation in the core reduction parameter

For stars of initially $16 M_\odot$, $18 M_\odot$, and $20 M_\odot$, we computed a series of models with different reduction parameters f (see Table 1). The evolutionary tracks in the HR diagram of these models are shown in Fig. 2, together with tracks for non-rotating Galactic stars from Brott et al. (2011) for $15 M_\odot$ and $20 M_\odot$.

Figure 2 reveals that the tracks in the HR diagram show discontinuous behaviour as a function of the parameter f . While at $16 M_\odot$, for example, the tracks vary little but in a systematic way for $f = 1.12$, 1.16 , and 1.18 , with slightly reduced main sequence widths and presupernova red supergiant luminosities for higher values of f , the track computed with $f = 1.20$ behaves qualitatively in a different way. Its main sequence part is still within the trend of the tracks with lower f -values, but during core helium burning, the model avoids the red supergiant regime, and it evolves into a presupernova configuration that is significantly more luminous than for the three other $16 M_\odot$ sequences.

Such discontinuous behaviour is also found at $18 M_\odot$ and $20 M_\odot$, although the jump occurs at different f -values. For the $18 M_\odot$ sequences, $f = 1.16$ still leads to a red supergiant configuration, whereas $f = 1.18$ and $f = 1.20$ does not. And in the $20 M_\odot$ models, the discontinuity is found between $f = 1.10$ and $f = 1.13$. If f were to measure the strength of the large scale magnetic field near the convective core boundary of our models,

less massive stars would require stronger fields in order to undergo core helium burning as a blue rather than a red supergiant.

The discontinuous behaviour also concerns the presupernova position of the models in the HR diagram. The models that burn helium as blue supergiants also end their evolution in this regime, while those that burn helium as red supergiants also die as such. Whether this remains true for intermediate values of f , which are not considered here, is not known. However, the $16 M_\odot$ model computed with $f = 0.20$ moves rather far towards the red supergiant regime after core hydrogen exhaustion and then turns around, such that the model burns helium as a red supergiant. It might thus be possible that models with f -values near the discontinuity have a brief red-supergiant phase before turning into core helium-burning red supergiants. Similarly, all our core helium-burning blue supergiant models evolve redwards during core helium burning. However, those that are still blue supergiants at core helium exhaustion will produce blue presupernova stars, since the models evolve mostly bluewards during their post-core helium-burning life time.

Our “magnetic” red supergiant presupernova stars have remarkably low luminosities, compared to stars computed with convective core overshooting, and their luminosity is smaller the larger their core reduction parameter f . This can be seen from Fig. 2, which shows the presupernova positions of our models in the HR diagram. For example, our “magnetic” $16 M_\odot$ models develop presupernova luminosities around $40\,000 L_\odot$, whereas the $16 M_\odot$ model of Brott et al. (2011) evolves into a presupernova red supergiant with a luminosity of $100\,000 L_\odot$. From Fig. 2 we conclude that our “magnetic” models would have to have a mass of about $22 M_\odot$ to produce such a luminous red supergiant presupernova model.

As expected, models with larger f -parameters develop lower core masses (Table 1). In fact, the CO cores of our “magnetic” $16 M_\odot$ models barely exceed the Chandrasekhar mass. This implies that, within our model assumptions, the limiting initial mass for neutron star formation depends on the strength of the large scale B field. For the range of core reduction parameters explored here, it would obviously not be found far below $16 M_\odot$. A similar shift may occur for the limiting initial mass for black hole formation.

Figure 3 shows the evolutionary tracks of models computed with a fixed value of the core reduction parameter f in the HR diagram, considering the mass range $16 M_{\odot}$ to $28 M_{\odot}$. Whereas the $16 M_{\odot}$ model evolves into a red supergiant at the beginning of core helium burning, the higher mass models all undergo core helium burning as blue supergiants. This confirms the trend that lower mass models require larger core reduction parameters in order to remain on the blue side of the HR diagram. Furthermore, for this fixed value of f , we find no significant trend in the effective temperature as a function of mass for our “magnetic” core helium-burning blue supergiants. Instead, all the models are found in the rather narrow effective temperature range of $T_{\text{eff}} \approx 17 \dots 23 \text{ kK}$. While there seems to be no strong trend with mass, this does not imply that all “magnetic” models would prefer this effective temperature range, as indicated, for example by our $16 M_{\odot}$ model computed with $f = 1.20$, which performs core helium burning at somewhat lower effective temperatures.

3.2. Comparison to previous models

While we are not aware of massive star evolutionary models with reduced convective cores due to internal large scale magnetic fields, models that arise from strong binary interactions can resemble our models to some extent. Considering the core helium-burning stage of evolution, the main feature of our “magnetic” models is that the helium core mass is significantly lower than that of ordinary stars with the same initial mass. This effect is also produced in some close binary models that simulate mass transfer, as well as in models for massive star mergers.

Braun & Langer (1995) simulated binary mass transfer by considering single stars that accreted considerable amounts of mass on a thermal time scale. They showed that, contrary to models using the Schwarzschild criterion for convection, the finite mixing time obtained when semiconvection is taken into account may prevent mass gainers from rejuvenating, if the accretion occurs late enough during its core hydrogen-burning phase. In such models, the convective core does not adapt to the new, higher mass, and thus the helium core mass in the later stages is significantly lower than that of ordinary stars. Braun & Langer (1995) found that for a given post accretion mass of $20 M_{\odot}$, a blue supergiant core helium-burning evolution was obtained when the helium core mass was lower than a certain mass limit. This is very analogous to the results we discuss in the previous section.

A similar result is obtained when mass transfer is initiated in a massive close binary just after core hydrogen exhaustion (Claeys et al. 2011), or in a massive binary merger that occurs after the more massive star has exhausted hydrogen in its core (Justham et al. 2014). For both situations, core helium-burning blue supergiant models are produced.

4. Comparison with observations

4.1. Main sequence stars

For the core hydrogen burning phase of evolution, the prime observable effect of our assumption that the large scale field leads to a lower convective core mass, is that the width of the main sequence band in the HR diagram is reduced compared to ordinary models. This effect is clearly visible in Fig. 3, which shows the position of the terminal age main sequence (TAMS) of our “magnetic” models and that of the non-rotating models of Brott et al. (2011).

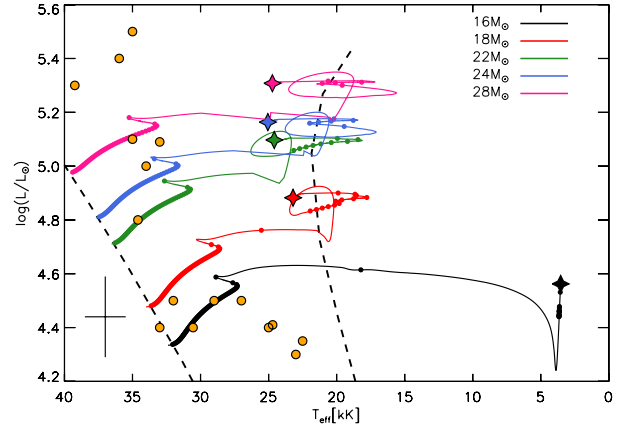


Fig. 3. HR diagram for stars between 16 and $28 M_{\odot}$ with convective cores reduced by the same factor, $f = 1.18$. Time steps for every 10^5 years are shown as small circles, starting at the end of the main sequence for clarity. The location of known massive magnetic main sequence stars (Briquet et al. 2013; Petit et al. 2013, and references therein; Alecian et al. 2014; Fossati et al. 2014, 2015; Neiner et al. 2014; Castro et al. 2015) are shown as yellow dots. Additionally, we draw the zero age and terminal age main sequences of the non-rotating models of Brott et al. (2011) as dashed lines.

Figure 3 also shows the positions of the known massive magnetic main sequence stars in the HR diagram. These stars are all Galactic objects. We find that the observed stars are not equally distributed within the main sequence band of the Brott models, but that, with some exceptions, they indeed concentrate in the area covered by the tracks of our “magnetic” models. We note that in a magnitude-limited sample, which roughly holds for the observed magnetic stars, one instead expects the cool side of the main sequence band to contain more stars than the hot side, since cool stars of the same luminosity are visually brighter. This remains true even when considering that for a constant magnetic flux, the magnetic field strength is less in more extended stars, and the field is thus harder to detect (Fossati et al. 2015). Alternatively, the distribution of the magnetic stars in Fig. 3 can also be explained by assuming that their B-field decays with a time scale close to or shorter than their evolutionary time scale (see again Fossati et al. 2015).

While this comparison does not give a final answer, it nevertheless shows that the assumption of magnetic stars having smaller convective cores than those of their non-magnetic counterparts leads to a possible interpretation of the data. In this context, it is interesting to mention that the convective core mass in massive stars may be measured directly through asteroseismology, as suggested by Mazumdar & Antia (2001) and Mazumdar et al. (2006). A comparative investigation of the convective core masses of magnetic and non-magnetic stars through asteroseismology by Briquet et al. (2007, 2012) indeed supports the idea that the magnetic stars do develop less massive cores.

If magnetic main sequence stars are really produced by the merging of two main sequence stars in a close binary system (Langer 2014), and the large scale field leads to smaller convective cores, then it is difficult to predict to what extent these objects will produce blue stragglers in star clusters (Schneider et al. 2015). Such stars are more luminous and bluer than the bulk of the main sequence stars, meaning that they are located beyond the turnoff point in the HR-diagram of the cluster. Even if the merged stars successfully rejuvenate, the subsequent suppression of the convective core mass may limit or even cancel the blue straggler effect; that is to say the magnetic main

sequence stars may or may not show up as blue stragglers. On the other hand, blue stragglers may also form from slower accretion events, which are less likely to give rise to large scale magnetic fields (Langer 2014). Thus, not all blue stragglers are expected to be magnetic stars.

The observational evidence for magnetic fields in blue stragglers is scarce, only about a dozen have been analysed so far. For roughly half of them magnetic fields were unambiguously detected (see for example Bagnulo et al. 2006). Other high-precision analyses could not confirm universal magnetic fields are present in blue stragglers (Fossati et al. 2010).

4.2. Supergiants

Figure 3 shows furthermore that our “magnetic” stars populate the region on the cool side of the TAMS of the non-magnetic models of Brott et al. In fact, while observationally, this region appears to be populated with stars (Fitzpatrick & Garmany 1990; Hunter et al. 2008; Vink et al. 2010), single star models generally do not spend any significant amount of time in this region (Ekström et al. 2012; Chieffi & Limongi 2013), such that the evolutionary history of the blue supergiants is in fact unclear at present (McEvoy et al. 2015).

Within the scope of the VLT-FLAMES Survey of Massive Stars, Evans et al. (2008), Hunter et al. (2008) and Vink et al. (2010) all find a steep drop in rotation rates at $\log g \approx 3.2$, as well as an increase in the surface nitrogen abundance. The quoted gravity defines the TAMS of the Brott et al. (2011) models around $15 M_{\odot}$. Both features have been recently confirmed within the VLT-FLAMES Tarantula Survey (Evans et al. 2011) by McEvoy et al. (2015). Our “magnetic” models do provide an explanation for the observed population with $\log g < 3.2$.

If the field in the magnetic main sequence stars does not decay, our models would then predict that the blue supergiants with $\log g < 3.2$ should exhibit a large scale magnetic field. Because their radii are larger by a factor of 3...10 and the main sequence stars show field strength of several hundred gauss (Petit et al. 2013; Fossati et al. 2015), flux conservation would lead to field strengths of the order of tens of gauss or less (for these stars see Fig. 3). These fields might thus be difficult to detect (Shultz et al. 2014).

As mentioned in Sect. 3.2, close binary evolution is also able to produce long-lived core helium-burning blue supergiants just adjacent to the TAMS. It would thus be interesting to investigate the binary fraction of the observed blue supergiants (Langer 2012). If they were produced by mass transfer or through a binary merger, detectable companion stars would hardly be expected (de Mink et al. 2014). The same would be true in the magnetic scenario if the large scale fields were really produced by strong binary interaction (cf., Sect. 1).

Finally, as shown by our models (Fig. 2), some magnetic stars with smaller cores may also evolve into red supergiants. We see two ways these might be observationally identified. One would be to look for the magnetic field itself. While flux conservation would lead to inhibitive small average surface field strengths, convection in the deep convective envelope might reorganise the field near the surface such that locally a much higher field strength could be possible. On the other hand, the deep convective envelopes of red supergiants may initiate a dynamo process that could lead to fields in all red supergiants (Dorch 2004). Indeed, Grunhut et al. (2010) find B fields in a third of the 30 massive cool supergiants that they investigated.

The other characteristic of our “magnetic” red supergiant models is their low luminosity-to-mass ratio. This could show up

in the photometry of young star clusters showing red supergiants which are dimmer than expected from the main sequence turn-off. Since the luminosity-to-mass ratio is thought to be proportional to the pulsation period in red supergiants (Gough et al. 1965; Heger et al. 1997), objects with low luminosity-to-mass ratios might also be identified through their pulsation properties.

4.3. Supernovae

When SN 1987A exploded in the LMC, it was a big surprise that the progenitor star turned out to be a blue supergiant (Walborn et al. 1989). While single-star models were produced soon thereafter that did predict blue supergiant progenitors (e.g. Woosley 1988; Saio et al. 1988; Langer et al. 1989), single-star models that include the OPAL opacities (Iglesias & Rogers 1996) do not appear to produce blue supergiant presupernova stars at the metallicity of the LMC.

As shown in Sect. 3, many of our “magnetic” models produce blue supergiant supernova progenitors. On the other hand, as discussed in Sect. 3.2, binary mass transfer and post main sequence merger may also produce blue presupernova stars. In this context it is interesting to note that other SN 1987A-like supernovae have been observed (e.g., Kleiser et al. 2011; Pastorello et al. 2012), and in fact Smartt et al. (2009) conclude that up to 3% of all supernovae could be of this type, meaning they have a blue progenitor star. Convective core suppression by large scale magnetic fields may help to explain such a large number of events.

4.4. Magnetars

Assuming flux freezing, the B field of the massive magnetic main sequence stars compressed to neutron star dimension would lead to the strength of magnetar fields (Ferrario & Wickramasinghe 2006). Indeed, if a massive main sequence stars had a B field of only $\sim 10^4$ G in their core, the resulting B field in the neutron star would be of the order of 10^{14} G, which is two orders of magnitude greater than typical neutron star magnetic field strengths (Langer 2014). In contrast to the scenario by Duncan & Thompson (1992), where the magnetar field forms from an extremely rapidly rotating collapsing iron core, magnetars as successors of magnetic main sequence stars would form slowly rotating neutron stars.

In the view of the idea that the magnetic fields in massive main sequence stars might be produced by strong binary interaction, Clark et al. (2014) propose that the blue hypergiant WD1-5 was the companion star of the magnetar J1647-45 in the young Galactic cluster Westerlund 1. To explain the unusual properties of WD1-5, in particular its high helium and carbon surface abundances, they propose that reverse mass transfer from the magnetar progenitor to WD1-5 must have occurred. This implies that WD1-5 was the initially more massive star and the original mass donor in the binary system, and that a strong accretion event could have formed a stable large scale field in the mass gainer. Clearly, a suppression of the convective core mass in the magnetar progenitor would have helped to obtain a supernova reversal, i.e. to have the initially less massive star explode first and produce the magnetar in this event.

5. Discussion and conclusions

We pursue the assumption that internal large scale magnetic fields in massive stars are capable of reducing the mass of their

convective cores during central hydrogen burning. While we are unable to quantitatively predict this effect, we take a parametric approach by assuming that effectively larger temperature gradients are needed to produce convection compared to the limit set by the Ledoux criterion (Gough & Tayler 1986). Indeed, the ability of magnetic fields to restrict convection is documented well for low-mass stars. The finding of Jackson et al. (2009) that the radii for low-mass M dwarfs in the young open cluster NGC 2516 are up to 50% larger than expected is reconciled well by MacDonald & Mullan (2013), who apply the Gough & Tayler criterion. Feiden & Chaboyer (2013, 2014), who model magnetic low-mass stars based on the technique developed by Lydon & Sofia (1985), confirm very similar behaviour by comparing them to detached eclipsing binaries.

We followed the evolution of stars in the mass range 16–28 M_{\odot} from the zero age main sequence roughly until neon ignition. Our ansatz allowed us to smoothly vary the extent of the core mass reduction and study its effects on the star's main sequence and post-main sequence evolution.

We showed that the stellar models obtained in this way predict various observational consequences. Their lower core masses compared to ordinary models lead to an earlier termination of the main sequence evolution, and to blue supergiant core helium-burning stars adjacent to the terminal age main sequence of ordinary stars. Both effects appear to be supported by observations, because the magnetic massive main sequence stars appear to prefer the hot side of the main sequence band, and the observed hot blue supergiants are not predicted by single-star evolution otherwise. Our models may also help to explain SN1987A-like supernovae, perhaps more abundantly than binary evolution.

On the other hand, binary evolution per se could produce the phenomenon of large scale stable B fields in a fraction of the massive main sequence stars, such as through stellar mergers. Multidimensional MHD calculations are required to investigate this question, and binary evolution models could then assess the effects of B fields on the further evolution in more detail.

Acknowledgements. We are grateful to Stephen Smartt and Henk Spruit for enlightening discussions. I.P. acknowledges support provided by DFG-grant LA 587/18. L.F. acknowledges financial support from the Alexander von Humboldt Foundation.

References

- Alecian, E., Kochukhov, O., Petit, V., et al. 2014, *A&A*, 567, A28
 Bagnulo, S., Landstreet, J. D., Mason, E., et al. 2006, *A&A*, 450, 777
 Bouret, J. C., Donati, J. F., Martins, F., et al. 2008, *MNRAS*, 389, 75
 Braithwaite, J. 2009, *MNRAS*, 397, 763
 Braithwaite, J., & Nordlund, Å. 2006, *A&A*, 450, 1077
 Braithwaite, J., & Spruit, H. C. 2004, *Nature*, 431, 819
 Braun, H., & Langer, N. 1995, *A&A*, 297, 483
 Briquet, M., Morel, T., Thoul, A., et al. 2007, *MNRAS*, 381, 1482
 Briquet, M., Neiner, C., Aerts, C., et al. 2012, *MNRAS*, 427, 483
 Briquet, M., Neiner, C., Leroy, B., Pápics, P. I., & MiMeS Collaboration 2013, *A&A*, 557, L16
 Brott, I., de Mink, S. E., Cantiello, M., et al. 2011, *A&A*, 530, A115
 Brun, A. S., Browning, M. K., & Toomre, J. 2005, *ApJ*, 629, 461
 Cantiello, M., & Braithwaite, J. 2011, *A&A*, 534, A140
 Cantiello, M., Langer, N., Brott, I., et al. 2009, *A&A*, 499, 279
 Castro, N., Fossati, L., Hubrig, S., et al. 2015, *A&A*, 581, A81
 Chieffi, A., & Limongi, M. 2013, *ApJ*, 764, 21
 Claeys, J. S. W., de Mink, S. E., Pols, O. R., Eldridge, J. J., & Baes, M. 2011, *A&A*, 528, A131
 Clark, J. S., Ritchie, B. W., Najarro, F., Langer, N., & Negueruela, I. 2014, *A&A*, 565, A90
 de Mink, S. E., Sana, H., Langer, N., Izzard, R. G., & Schneider, F. R. N. 2014, *ApJ*, 782, 7
 Donati, J.-F., & Landstreet, J. D. 2009, *ARA&A*, 47, 333
 Donati, J. F., Babel, J., Harries, T. J., et al. 2002, *MNRAS*, 333, 55
 Donati, J. F., Howarth, I. D., Bouret, J. C., et al. 2006, *MNRAS*, 365, L6
 Dorch, S. B. F. 2004, *A&A*, 423, 1101
 Dufton, P. L., Langer, N., Dunstall, P. R., et al. 2013, *A&A*, 550, A109
 Duncan, R. C., & Thompson, C. 1992, *ApJ*, 392, L9
 Ekström, S., Georgy, C., Eggenberger, P., et al. 2012, *A&A*, 537, A146
 Evans, C., Hunter, I., Smartt, S., et al. 2008, *The Messenger*, 131, 25
 Evans, C. J., Taylor, W. D., Hénault-Brunet, V., et al. 2011, *A&A*, 530, A108
 Featherstone, N. A., Browning, M. K., Brun, A. S., & Toomre, J. 2009, *ApJ*, 705, 1000
 Feiden, G. A., & Chaboyer, B. 2012, *ApJ*, 761, 30
 Ferrario, L., & Wickramasinghe, D. 2006, *MNRAS*, 367, 1323
 Fitzpatrick, E. L., & Garmany, C. D. 1990, *ApJ*, 363, 119
 Fossati, L., Mochneck, S., Landstreet, J., & Weiss, W. 2010, *A&A*, 510, A8
 Fossati, L., Zwintz, K., Castro, N., et al. 2014, *A&A*, 562, A143
 Fossati, L., Castro, N., Morel, T., et al. 2015, *A&A*, 574, A20
 Galloway, D. J., & Weiss, N. O. 1981, *ApJ*, 243, 945
 García-Berro, E., Lorén-Aguilar, P., Aznar-Siguán, G., et al. 2012, *ApJ*, 749, 25
 Glebbeek, E., Gaburov, E., Portegies Zwart, S., & Pols, O. R. 2013, *MNRAS*, 434, 3497
 Gough, D. O., & Tayler, R. J. 1966, *MNRAS*, 133, 85
 Goun, D. O., Ostriker, J. P., & Stobie, R. S. 1965, *ApJ*, 142, 1649
 Grunhut, J. H., Wade, G. A., Marcolino, W. L. F., et al. 2009, *MNRAS*, 400, L94
 Grunhut, J. H., Wade, G. A., Hanes, D. A., & Alecian, E. 2010, *MNRAS*, 408, 2290
 Grunhut, J. H., Wade, G. A., & MiMeS Collaboration 2012, in *AIP Conf. Ser.* 1429, eds. J. L. Hoffman, J. Bjorkman, & B. Whitney, 67
 Heger, A., Jeannin, L., Langer, N., & Baraffe, I. 1997, *A&A*, 327, 224
 Heger, A., Woosley, S. E., & Spruit, H. C. 2005, *ApJ*, 626, 350
 Hubrig, S., Schöller, M., Ilyin, I., et al. 2013, *A&A*, 551, A33
 Hubrig, S., Fossati, L., Carroll, T. A., et al. 2014, *A&A*, 564, L10
 Hunter, I., Lennon, D. J., Dufton, P. L., et al. 2008, *A&A*, 479, 541
 Iglesias, C. A., & Rogers, F. J. 1996, *ApJ*, 464, 943
 Jackson, R. J., Jeffries, R. D., & Maxted, P. F. L. 2009, *MNRAS*, 399, L89
 Justham, S., Podsiadlowski, P., & Vink, J. S. 2014, *ApJ*, 796, 121
 Kaper, L., Henrichs, H. F., Fullerton, A. W., et al. 1997, *A&A*, 327, 281
 Kleiser, I. K. W., Poznanski, D., Kasen, D., et al. 2011, *MNRAS*, 415, 372
 Köhler, K., Langer, N., de Koter, A., et al. 2015, *A&A*, 573, A71
 Kudritzki, R. P., Urbaneja, M. A., Bresolin, F., et al. 2008, *ApJ*, 681, 269
 Langer, N. 1991, *A&A*, 252, 669
 Langer, N. 2012, *ARA&A*, 50, 107
 Langer, N. 2014, in *IAU Symp.* 302, 1
 Langer, N., Fricke, K. J., & Sugimoto, D. 1983, *A&A*, 126, 207
 Langer, N., El Eid, M. F., & Baraffe, I. 1989, *A&A*, 224, L17
 Lydon, T. J., & Sofia, S. 1995, *ApJS*, 101, 357
 MacDonald, J., & Mullan, D. J. 2013, *ApJ*, 765, 126
 MacGregor, K. B., & Cassinelli, J. P. 2003, *ApJ*, 586, 480
 Mac Low, M. M., Balsara, D. S., Kim, J., & de Avillez, M. A. 2005, *ApJ*, 626, 864
 Mazumdar, A., & Antia, H. M. 2001, *A&A*, 377, 192
 Mazumdar, A., Briquet, M., Desmet, M., & Aerts, C. 2006, *A&A*, 459, 589
 McEvoy, C. M., Dufton, P. L., Evans, C. J., et al. 2015, *A&A*, 575, A70
 Mosser, B., Goupil, M. J., Belkacem, K., et al. 2012, *A&A*, 548, A10
 Neiner, C., Tkachenko, A., & MiMeS Collaboration 2014, *A&A*, 563, L7
 Nieuwenhuijzen, H., & de Jager, C. 1990, *A&A*, 231, 134
 Pastorello, A., Pumo, M. L., Navasardyan, H., et al. 2012, *A&A*, 537, A141
 Petit, V., Owocki, S. P., Wade, G. A., et al. 2013, *MNRAS*, 429, 398
 Prinja, R. K., & Howarth, I. D. 1988, *MNRAS*, 233, 123
 Royer, F., Zorec, J., & Gómez, A. E. 2007, *A&A*, 463, 671
 Saio, H., Nomoto, K., & Kato, M. 1988, *Nature*, 334, 508
 Sana, H., de Mink, S. E., de Koter, A., et al. 2012, *Science*, 337, 444
 Schatten, K. H., & Sofia, S. 1981, *Astrophys. Lett.*, 21, 93
 Schneider, F. R. N., Izzard, R. G., Langer, N., & de Mink, S. E. 2015, *ApJ*, 805, 20
 Shultz, M., Wade, G. A., Petit, V., et al. 2014, *MNRAS*, 438, 1114
 Smartt, S. J., Eldridge, J. J., Crockett, R. M., & Maund, J. R. 2009, *MNRAS*, 395, 1409
 Spruit, H. C. 2002, *A&A*, 381, 923
 Suijs, M. P. L., Langer, N., Poelarends, A.-J., et al. 2008, *A&A*, 481, L87
 Tayler, R. J. 1986, *MNRAS*, 220, 793
 Vink, J. S., de Koter, A., & Lamers, H. J. G. L. M. 2000, *A&A*, 362, 295
 Vink, J. S., Brott, I., Gräfener, G., et al. 2010, *A&A*, 512, L7
 Walborn N. R., Prevot M. L., Prevot L., et al. 1989, *A&A*, 219, 229
 Woosley, S. E. 1988, *ApJ*, 330, 218
 Yoon, S.-C., Langer, N., & Norman, C. 2006, *A&A*, 460, 199
 Zahn, J. P. 2009, *Commun. Asteroseismol.*, 158, 27
 Zahn, J. P. 2011, in *IAU Symp.* 272, eds. C. Neiner, G. Wade, G. Meynet, G. Peters, 14
 Zaussinger, F., & Spruit, H. C. 2013, *A&A*, 554, A119